


COMMUNICATION

Open Access



Sustainable and invisible anti-counterfeiting inks based on waterborne polyurethane and upconversion nanoparticles for leather products

Jun Xiang^{1*} , Jianxun Lin¹, Zhonghui Wang¹, Shenglin Zhou¹, Zhenya Wang¹, Qiang Yan^{2*}, Yidong Liu³ and Haojun Fan^{1*}

Abstract

Counterfeit leather products infringe the intellectual property rights of the business, cause enormous economic loss, and negatively influence the business enthusiasm for innovation. However, traditional anti-counterfeiting materials for leather products suffer from complicated fabrication procedures, photobleaching, and high volatile organic compound (VOC) emissions. Here, a sustainable and invisible anti-counterfeiting ink composed of waterborne polyurethane and water-dispersible lanthanide-doped upconversion nanoparticles (UCNPs) featuring ease of preparation, high photostability, non-toxicity, low VOC emissions, and strong adhesion strength for leather products is designed and synthesized. After decorating on the surface of leather products, the obtained patterns are invisible under normal light conditions. Upon irradiation at 808 nm, the invisible patterns can be observed by naked eyes due to the visible light emitted by 808 nm excited UCNPs. Our approach described here opens a new pathway to realize the long-term, stable anti-counterfeiting function of leather products.

Keywords: Sustainable, Invisible anti-counterfeiting, Waterborne polyurethane, Upconversion nanoparticles, Near-infrared light

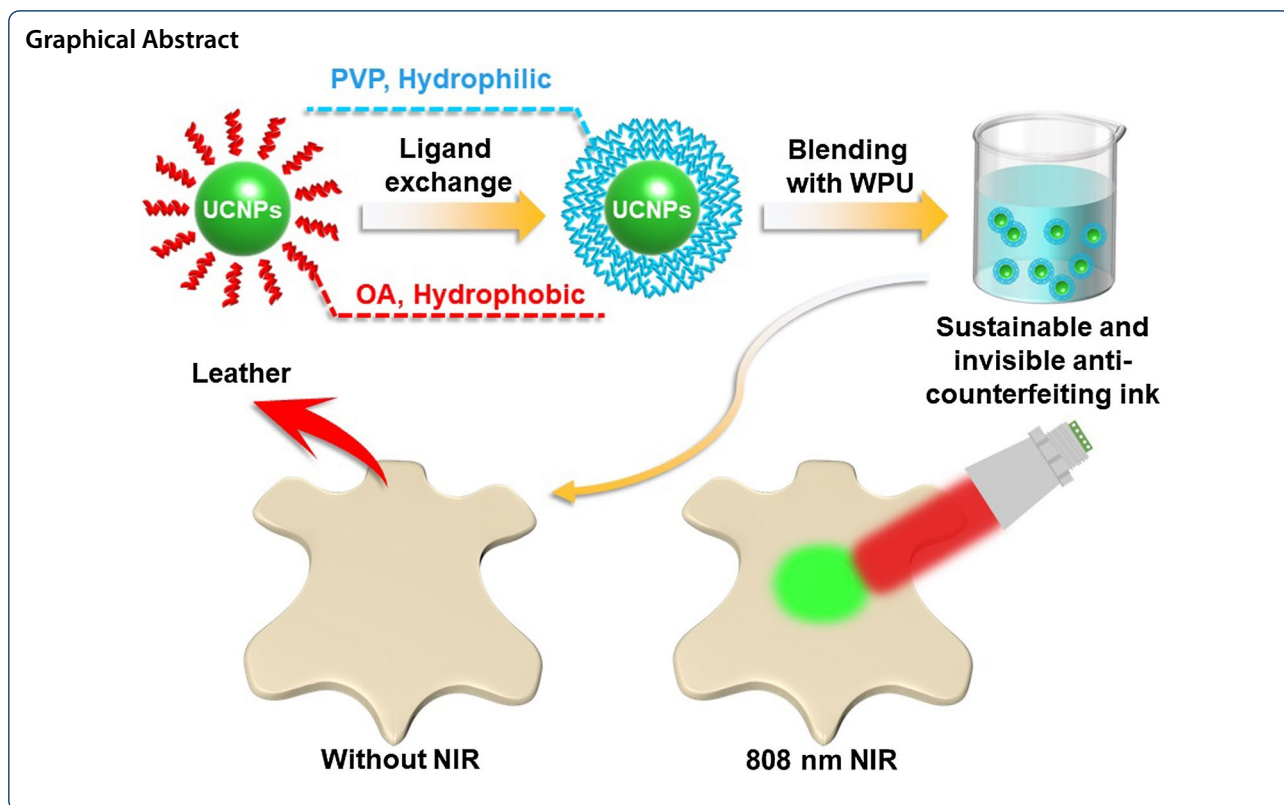
*Correspondence: junxiang@scu.edu.cn; yanq@fudan.edu.cn; fanhaojun@scu.edu.cn

¹ College of Biomass Science and Engineering, Key Laboratory of Leather Chemistry and Engineering of Ministry of Education, National Engineering Research Center of Clean Technology in Leather Industry, State Key Laboratory of Polymer Materials Engineering, Sichuan University, Chengdu 610065, People's Republic of China

² State Key Laboratory of Molecular Engineering of Polymers, Department of Macromolecular Science, Fudan University, Shanghai 200433, People's Republic of China

Full list of author information is available at the end of the article





1 Introduction

Nowadays, an increasing number of counterfeit leather products are arising in the market. To obtain high profits, some illegal traders counterfeit all kinds of best-selling leather products, which infringes the intellectual property rights of the business, causes huge economic loss, and negatively influences the business enthusiasm for innovation [1–3]. So far, anti-counterfeiting technology has been an effective method to curb the spread of counterfeit products. However, the traditional anti-counterfeiting technologies ranging from watermarks [4], holography [5–7], and two-dimensional barcodes [8], are difficult to reach the effective anti-counterfeiting purpose due to the simple preparation process and visible patterns. Invisible anti-counterfeiting materials have attracted the attention of researchers by their high concealment properties [9–11]. The most frequently used invisible anti-counterfeiting technology in leather products is to draw invisible anti-counterfeiting labels (ACLs) with organic fluorescent dyes [12]. Generally, such labels suffer from short service life due to the photobleaching of organic dyes under irradiation [13, 14]. One way to address this issue is to use fluorescent inorganic nanomaterials to prepare these invisible ACLs [15–17], e.g., quantum dots. However, they are toxic [13] and often require ultraviolet (UV) photons to achieve the

anti-counterfeiting function. It is well known that UV light may cause the degradation of organic materials in the ACLs and shorten their service life [18–20]. Therefore, searching for a non-toxic inorganic material having good luminescent stability to prepare ACLs remains a grand challenge.

As a competitive alternative, lanthanide-doped upconversion nanoparticles (UCNPs), capable of converting invisible low-energy near-infrared (NIR) photons into visible photons via a nonlinear optical process [21–25], are excellent candidates for preparing the invisible ACLs [10, 11, 26–30]. The main reasons are described as follows. First, UCNPs are inorganic nanocrystals and have high luminescent stability compared with organic fluorescent dyes [20, 31]. This indicates that the service life of the ACLs prepared by UCNPs is expected to be longer than that prepared by organic fluorescent dyes. Second, UCNPs are non-toxic and have no harmful health effects on people [20, 32, 33]. Third, UCNPs use the NIR light as the excitation source. Compared with high-energy UV and visible light, low-energy NIR light does not harm the organic materials in the ACLs [19, 34, 35]. Fourth, lanthanide ions exhibit narrow half-peak width. Thus, the emission color of UCNPs is pure and easy to be caught by naked eyes [36]. Given the above UCNPs nature, some

researchers have utilized UCNPs to prepare upconversion luminous printing ink. For example, Blumenthal and his colleagues proposed a NIR-responsive invisible upconversion ink [37]. The basic idea was to blend UCNPs (β -NaYF₄:3%Er,17%Yb) and poly(methyl methacrylate) in the mixture of toluene and methyl benzoate to form an invisible ink. After that, direct writing and screen printing were used to make invisible marks on the Kapton[®], glass slides, and high bond paper. Despite such progress, surprisingly, there is no report on exploiting UCNPs to prepare invisible ACLs for leather products.

Here, we demonstrate a facile strategy to utilize UCNPs to construct invisible ACLs for leather products. To achieve this goal, we must solve two problems. First, water-dispersible UCNPs are needed. In general, UCNPs with excellent luminescence properties are synthesized by the solvothermal method [21, 38, 39]. The as-prepared UCNPs are often capped with oleic acid (OA-UCNPs) on their surface, limiting their dispersity only in low polarity organic solvents [24, 27, 40]. However, increasingly factories are using water, a greener and safer solvent, to replace organic solvents in their manufacture due to the enhanced environmental protection awareness and environmental regulation policies of the government [41]. Thus, our first step is to impart water dispersity to OA-UCNPs. Second, how to improve the adhesion between UCNPs and leather products? Generally, OA-UCNPs have poor adhesion to leather products and lead to short service life. Waterborne polyurethane (WPU) is an excellent adhesive for various uses, including leather finishing, fabric coating, paint, and surface treatment agents [42–46]. Its unique advantages, such as environmentally friendly, good mechanical properties, high safety, excellent compatibility, and easy modification. Therefore, invisible ACLs prepared by water-dispersible UCNPs integrated with WPU may significantly enhance the adhesion between UCNPs and leather products.

As a proof-of-concept, here we develop a novel anti-counterfeiting ink (ACI) comprising water-dispersible UCNPs and WPU for leather products. First, hydrophobic OA-UCNPs are transformed into polyvinylpyrrolidone capped UCNPs (PVP-UCNPs) by ligand exchange at room temperature. Afterward, PVP-UCNPs and synthesized WPU are blended to form a sustainable and invisible environmental-friendly ACI. Finally, this elaborately designed ink is coated on the leather substrate to obtain ACLs. By design, the label is invisible without 808 nm NIR irradiation. In contrast, upon 808 nm NIR illumination, the label emits green light, capable of catching by naked eyes, realizing the effectively invisible anti-counterfeiting function of leather products. In addition, the coating layer remains stable on leather products

even after abrasion and tape-peeling tests, indicating the excellent durability of the prepared ACL.

2 Materials and methods

2.1 Materials

Polypropylene glycol (PPG, $M_n=1,000$ g/mol), isophorone diisocyanate (IPDI), 1,4-butanediol (BDO), trimethylolpropane (TMP), 2,2-bis(hydroxymethyl) propionic acid (DMPA), and bismuth acid catalyst were supplied by Dymatic Post Polymer Material Co. (Lishui, China). Methanol (99.9%), ethanol (99.9%), hexane (99.5%), acetone (AR), *N,N*-dimethylformamide (DMF, AR), dichloromethane (DCM, AR), Di-*n*-butylamine (AR), triethylamine (AR), ethylenediamine (AR), Polyvinylpyrrolidone (PVP, $M_w=8,000$ – $12,000$ g/mol) were purchased from Kelong Chemical Engineering Co. Ltd. (Chengdu, China). Oleic acid capped 808 nm-excitable core-shell-shell NaYF₄:18%Yb,2%Er@NaNdF₄:10%Yb@NaYF₄ upconversion nanoparticles, OA-UCNPs, were synthesized using the solvothermal method as previously reported by our group [47].

2.2 Experimental methods

2.2.1 Synthesis of waterborne polyurethane (WPU)

First, 40.0 g PPG was placed in a four-neck round-bottom flask and dehydrated in a vacuum oven at 120 °C for 2 h. When it was cooled down to 70 °C, 31.00 g IPDI and 0.10 g bismuth acid catalyst were added to it. This mixture was stirred vigorously under nitrogen gas protection, then slowly heated to 85 °C for 1 h. After that, 1.00 g TMP, 2.60 g BDO, and 3.90 g DMPA were added and stirred for another 3 h. Subsequently, this solution was cooled down to 40 °C and 3.82 g triethylamine was added to neutralize the free carboxylic groups for 4 h. Finally, a WPU emulsion with around 30 wt% solid content was obtained after emulsification for 30 min with 183.0 g deionized water and chain extension reaction for 1 h using 1.75 g ethylenediamine under vigorous stirring.

2.2.2 Preparation of polyvinylpyrrolidone capped upconversion nanoparticles (PVP-UCNPs)

PVP modified upconversion nanoparticles, PVP-UCNPs, were prepared based on the method described in our previously published work [24]. First, 57 mg NOBF₄ was dissolved in a mixture of DMF (2.23 mL) and DCM (57.30 mL). Second, OA-UCNPs (190 mg) in 15 mL of hexane were added to it and the resulting mixture was shaken violently for 5 min. Third, this solution was centrifuged (10,000 rpm, 10 min) and the precipitate was collected, washed with a mixture of DMF and DCM, and redispersed in 8 mL of DMF. Fourth, 7 mL of this dispersion and 85 mg PVP in 1 mL H₂O were mixed and stirred vigorously for 3 h at room temperature.

Hereafter, PVP-UCNPs were obtained by centrifugation and washed with water ($2\times$). Finally, PVP-UCNPs were redispersed in water (8.40 mg/mL) before use.

2.2.3 Preparation of the sustainable and invisible anti-counterfeiting ink (ACI)

Briefly, the mixture of PVP-UCNPs (1 mL, 8.40 mg/mL) and WPU (3 mL, solid content = ~ 30 wt%) was stirred at room temperature for 10 min. Then, it was defoamed under sonication to obtain the ACI with a solid content of ~ 23 wt% (WPU:PVP-UCNPs weight ratio 107:1). This sustainable and invisible ACI was kept at room temperature before use.

2.3 Measurements

2.3.1 Attenuated total reflection fourier transform infrared spectroscopy (ATR-FTIR)

ATR-FTIR spectra were acquired on a Nicolet IS50 FTIR spectrometer using transmission mode. Spectra were obtained in the region of $4000-400\text{ cm}^{-1}$ at a resolution of 4 cm^{-1} .

2.3.2 X-ray diffraction (XRD)

Powder X-ray diffraction measurements were performed on an XRF-1800 instrument with a flat sample holder and the Cu-K α radiation ($\lambda = 1.54\text{ \AA}$) in the 2θ range from 10° to 70° with 40 kV operating voltage and 40 mA current.

2.3.3 Transmission electron microscope (TEM)

Typically, 15 μL OA-UCNPs solution was dropped onto the surface of carbon-coated copper grids (Beijing XXBR Technology Co., Ltd, T11023). After hexane completely evaporated, the aqueous phosphotungstic acid solution (1 wt%) was used for staining. Finally, TEM images were collected by a HT7700 Hitachi microscopy at the accelerating voltage of 200 kV.

2.3.4 Upconversion emission spectra

The upconversion emission spectra of all samples were measured by a Hitachi F-7100 Spectrophotometer. A continuous-wave diode NIR laser (808 nm) was employed as the excitation source.

2.3.5 Scanning electron microscope (SEM)

The sustainable and invisible ACI composed of PVP-UCNPs and WPU was coated on the surface of leather products. After that, all samples were sprayed with gold after drying completely. Finally, SEM images were collected by a JSM-7500F scanning electron microscope.

2.3.6 Dynamic light scattering (DLS)

DLS studies were performed with a Malvern Zetasizer Nano ZS ZEN3600 system equipped with a helium–neon

laser ($\lambda = 633\text{ nm}$) at a scattering angle of 173° . Samples are diluted before attempting a DLS size test.

2.3.7 Abrasion resistance test

Abrasion resistance of the ACLs was determined by the Taber abrader (XK-3017, Xiangke Testing Instrument Co., Ltd.) instrument. The digital pictures were taken after ACLs were rubbed for 500 cycles, 1,000 g weight load at 60 RPM.

2.3.8 Adhesion strength test

The adhesion was investigated by a tape test. A 3 M scotch tape was utilized to attach onto samples and then peeled off from them. The test was repeated 3 times.

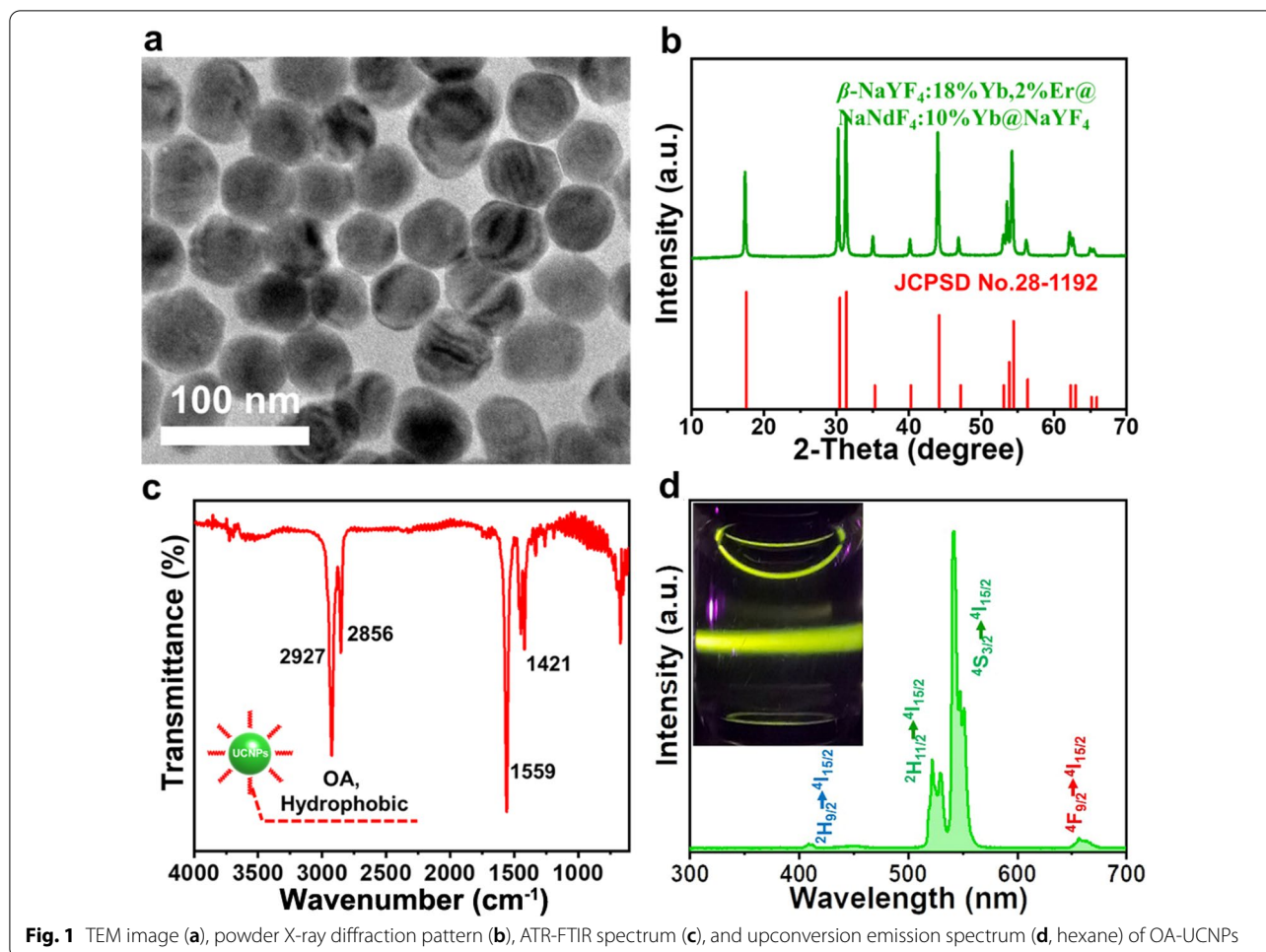
3 Results and discussion

3.1 OA-UCNPs nanoparticles

In our first step, we synthesized OA-UCNPs nanocrystals. Figure 1a shows that their size is around $55\text{ nm} \times 45\text{ nm}$ (length \times width) and they have a high degree of monodispersity. Morphologies and phase structures have a significant impact on their upconversion luminescent properties. The hexagonal phase UCNPs are preferred because they possess high upconversion luminescence efficiency [48–50]. Furthermore, the crystal structure of OA-UCNPs was tested by XRD studies. As shown in Fig. 1b, all diffraction peaks of OA-UCNPs are in good agreement with the standard hexagonal β crystal pattern. The diffraction peaks of the OA-UCNPs are strong and sharp, suggesting that these nanocrystals have a high degree of crystallinity.

The ATR-FTIR spectrum of OA-UCNPs is shown in Fig. 1c. Two strong absorption peaks appear at 2927 cm^{-1} and 2856 cm^{-1} , corresponding to the symmetric stretching vibration absorption peak and asymmetric stretching vibration absorption peak of methylene (CH_2) in the molecular structure of OA, respectively. The asymmetric and symmetric stretching vibration absorption peaks of the carboxyl group (COOH) in oleic acid molecules are observed at 1559 cm^{-1} and 1421 cm^{-1} , respectively. Besides, the bending vibration bond of the C-H usually appears at 1420 cm^{-1} , which overlaps the absorption peak of the carboxyl group. It can be concluded that there are OA molecules on the surface of UCNPs.

Figure 1d shows the upconversion emission spectrum of OA-UCNPs under 808 nm NIR irradiation. As can be seen, OA-UCNPs emitted photons in the visible light region. These emission peaks at 409 nm, 521 nm, 542 nm, and 653 nm could be assigned to the transitions of Er^{3+} from the excited state levels of ${}^2\text{H}_{9/2}$, ${}^2\text{H}_{11/2}$, ${}^4\text{S}_{3/2}$, and ${}^4\text{F}_{9/2}$ to the ground state level of ${}^4\text{I}_{15/2}$, respectively. In addition, a photograph of OA-UCNPs in hexane is inserted into Fig. 1d. There was a bright green

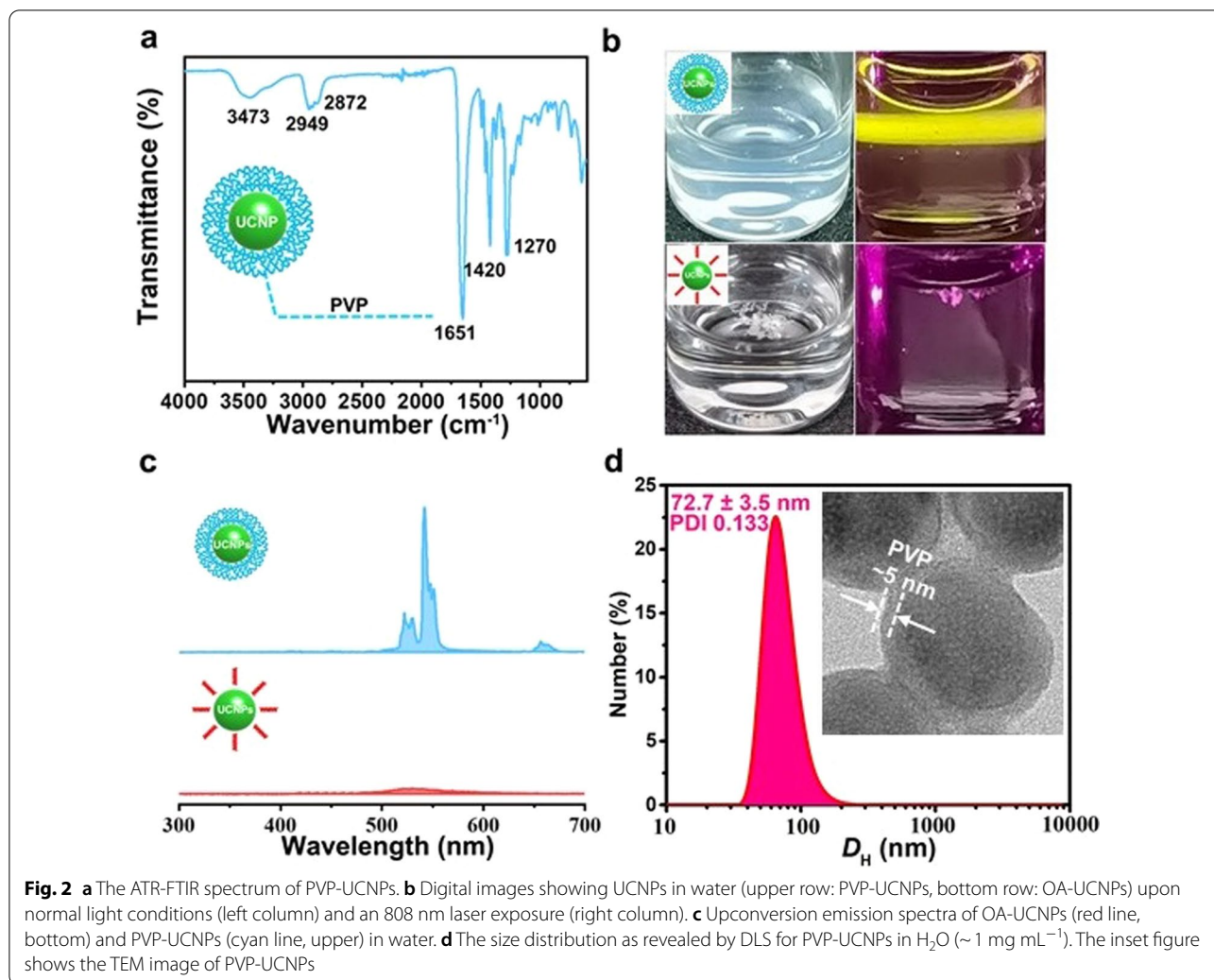


light column caught by naked eyes where the 808 nm NIR light passed through the solution. All above results indicate that the OA-UCNPs featuring a high degree of uniformity, crystallinity with β crystal phase as well as excellent luminescent properties have been successfully synthesized.

3.2 PVP-UCNPs nanoparticles

In this work, we aim to use water, a greener and safer solvent, to replace the volatile organic solvent (hexane) of UCNPs. To this end, OA-UCNPs were rendered with water dispersibility via the ligand exchange method using a hydrophilic polymer, PVP, according to previously reported works [24, 40]. To verify the successful surface modification, Fig. 2a exhibits the ATR-FTIR spectrum of obtained PVP-UCNPs. As expected, the characteristic absorption peaks of OA molecules are absent. Meanwhile, the absorption peaks at 1651 cm^{-1} and 1270 cm^{-1} are attributed to the stretching vibration of C=O and the bending vibration of C-N in PVP, indicating that the existence of PVP polymer.

After removing OA molecules, UCNPs can easily disperse in water (Fig. 2b, upper-left corner). By contrast, in water, we found that OA-UCNPs formed aggregates (Fig. 2b, bottom-left corner) due to the hydrophobic nature of OA molecules. In addition, there is no green light emitted from UCNPs when the laser passes through the solution (Fig. 2b, bottom-right corner). Compared with those of OA-UCNPs, the emission bands of PVP-UCNPs (Fig. 2c, upper) resembling those of OA-UCNPs (Fig. 1d) were observed. Furthermore, an apparent light beam in the PVP-UCNPs aqueous solution appeared when the dispersion was exposed to the 808 nm laser (Fig. 2b, upper-right corner). This phenomenon can be attributed to the upconversion luminescence of PVP-UCNPs aqueous solution under illumination. In addition, the average hydrodynamic diameter (D_H) of PVP-UCNPs is around 72.7 nm and these nanoparticles have a relatively high degree of monodispersity in H_2O (Fig. 2d). TEM image shows that the average thickness of the PVP layer is about 5 nm (the inset in Fig. 2d). Our findings clearly indicate



that PVP-UCNPs with excellent water dispersibility have been successfully prepared.

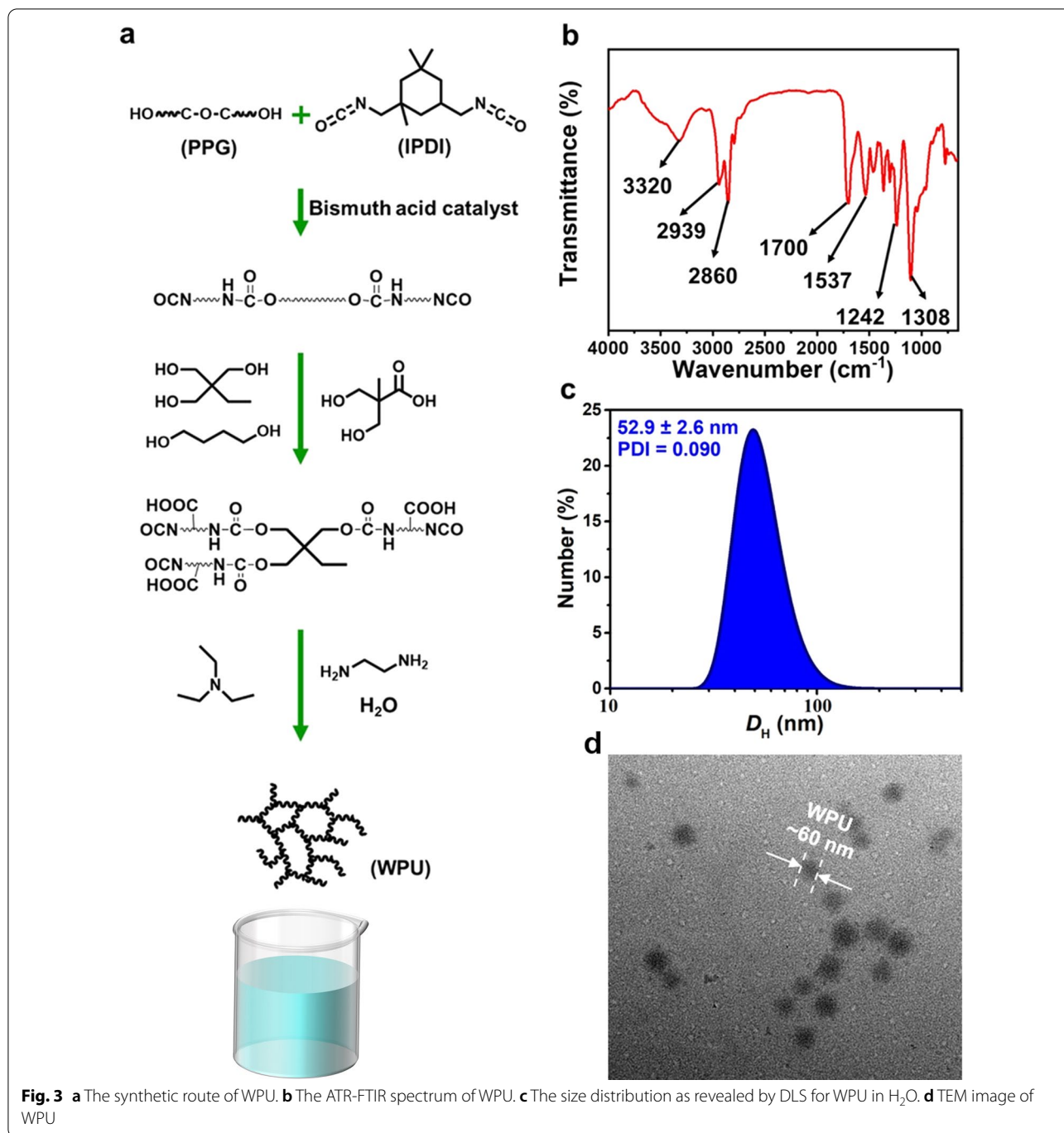
3.3 The WPU dispersion

The synthetic route of WPU is shown in Fig. 3a. ATR-FTIR measurement was conducted to verify its successful synthesis. In Fig. 3b, the disappearance of characteristic absorption peak at 2270 cm⁻¹ indicates that isocyanate (-NCO) groups have been completely consumed. Several new peaks appear at 3323 cm⁻¹, 1700 cm⁻¹, and 1537 cm⁻¹ belonging to the stretching vibration absorption of -N-H, -C=O, and -C-N-, respectively, implying the existence of carbamate groups. In addition, the peaks at 1242 cm⁻¹ and 1308 cm⁻¹ are the -C-O- stretching vibration peak of carbamate groups and -C-O-C- stretching vibration peak in the molecular skeleton of PPG, respectively. Furthermore, the DLS test ($D_H = 52.9 \pm 2.6$ nm, PDI = 0.090, Fig. 3c) and TEM observations (spherical shapes, Fig. 3d)

indicate that WPU has a high degree of monodispersity. All observations confirm that WPU has been successfully synthesized.

3.4 The sustainable and invisible ACI

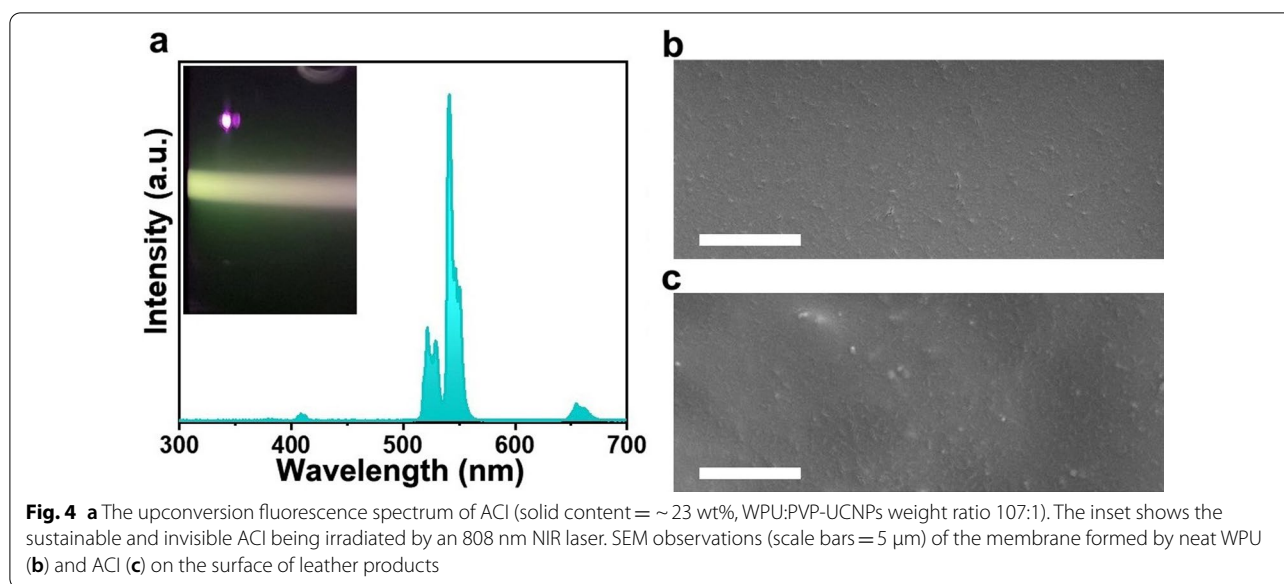
Next, the luminescent property of PVP-UCNPs blended with WPU, namely ACI, was investigated. Similarly, upon exposure to the 808 nm laser, an obvious light beam was found in the ACI solution (the inset in Fig. 4a). In addition, all emission peaks of ACI are in good agreement with OA-UCNPs in hexane, which indicates that WPU has a negligible effect on the emission property of UCNPs. We further detect the dispersibility of PVP-UCNPs within the WPU matrix. Thin films formed by the ACI and WPU were coated on the leather's surface by roller coating. Figure 4b, c show that UCNPs disperse very well in the WPU membrane, suggesting that PVP-UCNPs have good compatibility with the designed WPU.



3.5 Application

In the final step, the invisible ACLs were drawn on the leather products' surface with the sustainable and invisible ACI (WPU:PVP-UCNPs weight ratio 107:1). In addition, the labels formed by the neat WPU ink were also drawn as control tests. As shown in Fig. 5a, the patterns painted with as-prepared ACI and neat WPU could not be observed by naked eyes under normal light conditions.

When an 808 nm laser irradiated them, the pattern made by ACI could be visualized in the dark due to the green light emitted from UCNPs in the label. In contrast, the pattern written by only WPU had no change under the laser illumination. We further evaluate its durability on the surface of leather products. Figure 5b shows that no shedding of nanoparticles was observed after abrasion 500 cycles. Meanwhile, the coated ACLs also exhibited



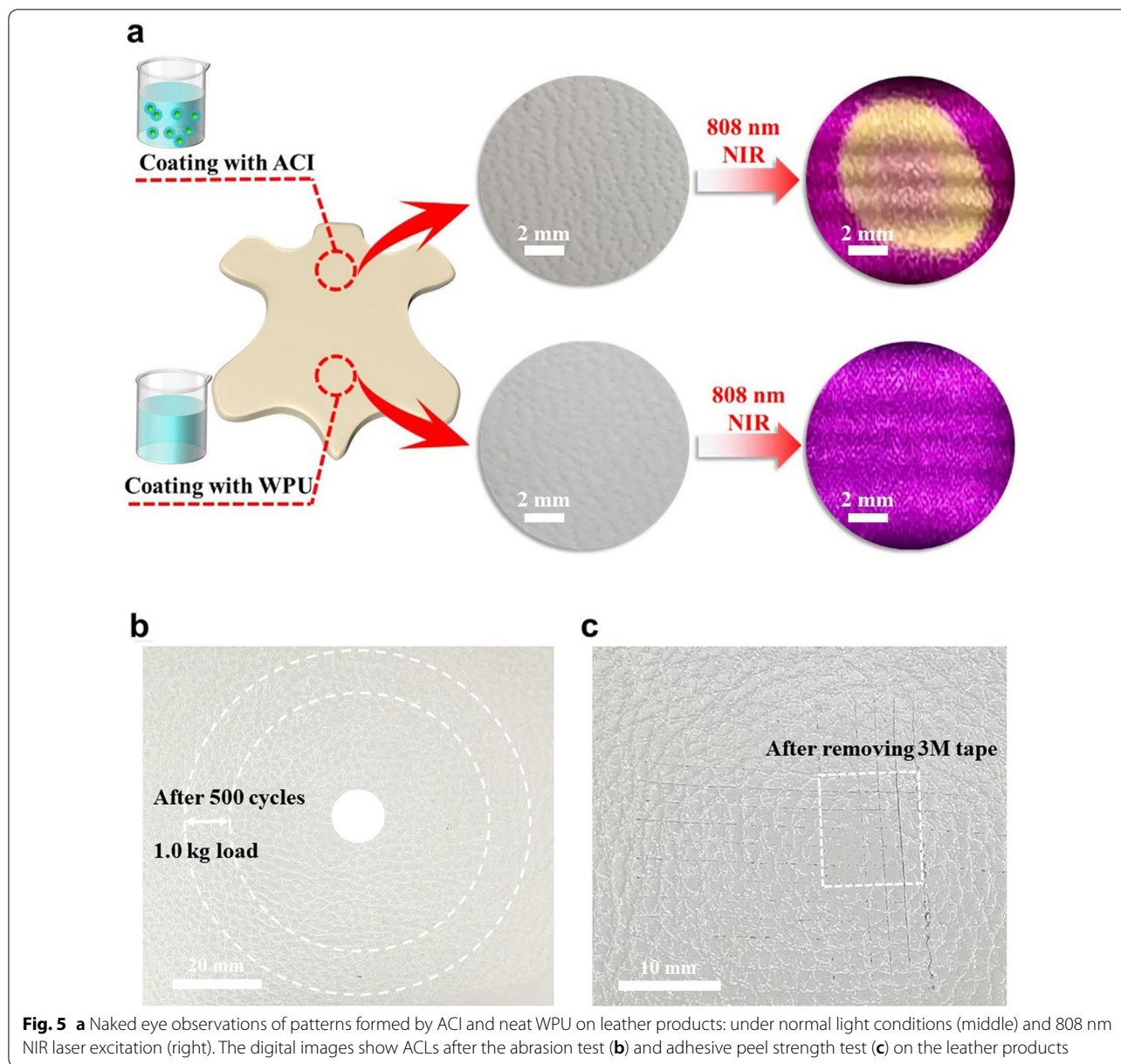
strong adhesive strength to the leather products (Fig. 5c). These results prove that the designed ink can serve as an excellent anti-counterfeiting ink for leather products.

The purpose of this work is to establish a facile and general strategy to combine UCNPs and WPU for realizing the anti-counterfeiting function of leather products. In practical applications, the proposed anti-counterfeiting technology must be hard to reverse engineer. Fortunately, we are delighted to see studies on UCNPs have witnessed rapid growth, especially in the past decade [51]. Owing to the luminescence tunability of UCNPs, mixing various types of UCNPs (e.g., NIR-to-blue UCNPs and NIR-to-green UCNPs) or employing advanced UCNPs (e.g., dual-excitation ones) can be an effective way to achieve a higher security level of such ACLs [29, 52]. As for the cost, the weight ratio of WPU and PVP-UCNPs is 107:1 in final ACLs. Considering the following aspects, such as the possible mass production of UCNPs [53], low prices of WPU (~3 USD per kilogram in this work), small coating area (below 1 cm^2) and 10~20 μm thin-film thickness of these ACLs on leather products, we believe that such an ACI is a competitive alternative to the traditional ones, not to mention their environmentally benign nature. Last but not the least, the end-of-life of the labeled leather is another issue that deserved to be discussed. Given continuous efforts have been made to the life cycle assessment of leather industry [54], here we narrow the scope of discussion into the recyclability of materials in ACLs, namely UCNPs and WPU. On the one hand, UCNPs are inorganic nanocrystals and more stable compared with

organic dyes. They can be recycled by dissolving with suitable solvents and readily re-collecting by centrifugation (the density of UCNPs is ca. 4.3 g cm^{-3}). On the other hand, among literatures, recyclable and high-performance WPU have been successfully designed and synthesized, e.g., by incorporating dynamic carboxylic metal ion interactions [55]. Therefore, the design and synthesis of ACLs composed of UCNPs and WPU with recyclability at the end of life are very likely.

4 Conclusions

In summary, we have reported a robust and straightforward method to prepare sustainable and invisible ACLs for leather products. First, 808 nm-excitable OA-UCNPs with excellent luminescent properties were prepared by the solvothermal method. Subsequently, we endowed them with hydrophilicity through the ligand exchange method by using PVP. After mixing it with an anionic WPU dispersion, the obtained mixture can act as an excellent ACI for leather products. Under normal light conditions, the ACLs formed by this mixture were invisible. By contrast, under 808 nm irradiation, the labels could be observed by naked eyes due to the emitted upconversion light. Given the high photostability, non-toxicity, low VOC emission, and good adhesive strength to leather products, we believe that this elaborately designed and synthesized anti-counterfeiting material made of WPU and UCNP can be a competitive alternative to traditional ones for leather products.



Acknowledgements

The project was financially supported by the National Natural Science Foundation of China (21905182), the Key Research and Development Program of Shandong Province (2019JZZY010355), the National Key Research and Development Program of China (2021YFC2101900), the Synthetic Leather and High-Performance fibers Innovation Team (2020SCUNG122), the Fundamental Research Funds for the Central Universities (YJ201940), and the 615 Talent Introduction Program of Jiangsu Dongtai for Leading Talents.

Authors' contributions

JX, QY, and HF supervised the project, conceived the original idea, designed the figures, revised the manuscript, and proof outline. JL drafted the manuscript. JL, ZW, ZW, SZ, and YL contributed to sample preparation and characterization. All authors discussed the results and finalized the manuscript.

Funding

National Natural Science Foundation of China (21905182); Key Research and Development Program of Shandong Province (2019JZZY010355); National Key Research and Development Program of China (2021YFC2101900); Synthetic Leather and High-Performance fibers Innovation Team (2020SCUNG122); 615 Talent Introduction Program of Jiangsu Dongtai for Leading Talents; Fundamental Research Funds for the Central Universities (YJ201940).

Availability of data and materials

All data generated or analyzed during this study are included in this published article.

Declarations

Competing interests

The authors declare that they have no competing interests.

Author details

¹College of Biomass Science and Engineering, Key Laboratory of Leather Chemistry and Engineering of Ministry of Education, National Engineering Research Center of Clean Technology in Leather Industry, State Key Laboratory of Polymer Materials Engineering, Sichuan University, Chengdu 610065, People's Republic of China. ²State Key Laboratory of Molecular Engineering of Polymers, Department of Macromolecular Science, Fudan University, Shanghai 200433, People's Republic of China. ³Dongtai City Fu'an Synthetize Material Co. Ltd., Yancheng, Jiangsu, People's Republic of China.

Received: 24 May 2021 Accepted: 25 November 2021

Published online: 15 December 2021

References

- Nguyen HP, Retraint F, Morain-Nicolier F, et al. A watermarking technique to secure printed matrix barcode-application for anti-counterfeit packaging. *IEEE Access*. 2019;7(1):1839–50.
- Smith AF, Skrabalak SE. Metal nanomaterials for optical anti-counterfeit labels. *J Mater Chem C*. 2017;5(13):3207–15.
- Kumar P, Singh S, Gupta BK. Future prospects of luminescent nanomaterial based security inks: from synthesis to anti-counterfeiting applications. *Nanoscale*. 2016;8(30):14297–340.
- Huang S, Wu JK. Optical watermarking for printed document authentication. *IEEE Trans Inf Forensics Secur*. 2007;2(2):164–73.
- Miao J, Ding X, Zhou S, et al. Fabrication of dynamic holograms on polymer surface by direct laser writing for high-security anti-counterfeit applications. *IEEE Access*. 2019;7:142926–33.
- Tate N, Nomura W, Yatsui T, et al. Hierarchical hologram based on optical near- and far-field responses. *Opt Express*. 2008;16(2):607–12.
- Lu YT, Chi S. Compact, reliable asymmetric optical configuration for cost-effective fabrication of multiplex dot matrix hologram in anti-counterfeiting applications. *Optik*. 2003;114(4):161–7.
- Li W-S, Shen Y, Chen Z-J, et al. Demonstration of patterned polymer-stabilized cholesteric liquid crystal textures for anti-counterfeiting two-dimensional barcodes. *Appl Opt*. 2017;56(3):601–6.
- Chen X, Wang Q, Wang X-J, et al. Synthesis and performance of ZnO quantum dots water-based fluorescent ink for anti-counterfeiting applications. *Sci Rep*. 2021;11(1):5841.
- Sangeetha NM, Moutet P, Lagarde D, et al. 3D assembly of upconverting NaYF₄ nanocrystals by AFM nanoxerography: creation of anti-counterfeiting microtags. *Nanoscale*. 2013;5(20):9587–92.
- Liu Y, Ai K, Lu L. Designing lanthanide-doped nanocrystals with both up- and down-conversion luminescence for anti-counterfeiting. *Nanoscale*. 2011;3(11):4804–10.
- Yoon B, Lee J, Park IS, et al. Recent functional material based approaches to prevent and detect counterfeiting. *J Mater Chem C*. 2013;1(13):2388–403.
- Yao W, Tian Q, Liu J, et al. Preparation and RGB upconversion optical properties of transparent anti-counterfeiting films. *Nanoscale*. 2017;9(41):15982–9.
- De Cremer G, Sels BF, Hotta J-I, et al. Optical encoding of silver zeolite microcarriers. *Adv Mater*. 2010;22(9):957–60.
- Freeman R, Willner I. Optical molecular sensing with semiconductor quantum dots (QDs). *Chem Soc Rev*. 2012;41(10):4067–85.
- Li H, He X, Kang Z, et al. Water-soluble fluorescent carbon quantum dots and photocatalyst design. *Angew Chem Int Ed*. 2010;49(26):4430–4.
- Resch-Genger U, Grabolle M, Cavaliere-Jaricot S, et al. Quantum dots versus organic dyes as fluorescent labels. *Nat Methods*. 2008;5(9):763–75.
- Ding B-B, Liu K, Zhang F, et al. Facile synthesis of β -NaGdF₄:Yb/Er@CaF₂ nanoparticles with enhanced upconversion fluorescence and stability via a sequential growth process. *CrystEngComm*. 2015;17(31):5900–5.
- Lee JB, Kim M. Photo-degradation of malachite green in mudfish tissues-investigation of UV-induced photo-degradation. *Food Sci Biotechnol*. 2012;21(2):519–24.
- Chatterjee DK, Rufaihah AJ, Zhang Y. Upconversion fluorescence imaging of cells and small animals using lanthanide doped nanocrystals. *Biomaterials*. 2008;29(7):937–43.
- Xiang J, Zhou S, Lin J, et al. Low-power near-infrared-responsive upconversion nanovectors. *ACS Appl Mater Interfaces*. 2021;13(6):7094–101.
- Xiang J, Tong X, Shi F, et al. Near-infrared light-triggered drug release from UV-responsive diblock copolymer-coated upconversion nanoparticles with high monodispersity. *J Mater Chem B*. 2018;6(21):3531–40.
- Xiang J, Ge F, Yu B, et al. Nanocomplexes of photolabile polyelectrolyte and upconversion nanoparticles for near-infrared light-triggered payload release. *ACS Appl Mater Interfaces*. 2018;10(24):20790–800.
- Xiang J, Tong X, Shi F, et al. Spatial organization and optical properties of layer-by-layer assembled upconversion and gold nanoparticles in thin films. *J Mater Chem C*. 2016;4(39):9343–9.
- Chen G, Qiu H, Prasad PN, et al. Upconversion nanoparticles: design, nanochemistry, and applications in theranostics. *Chem Rev*. 2014;114(10):5161–214.
- Zhang C, Li X, Liu M, et al. Dual-wavelength stimuli and green emission response in lanthanide doped nanoparticles for anti-counterfeiting. *J Alloys Compounds*. 2020;836:155487.
- You M, Zhong J, Hong Y, et al. Inkjet printing of upconversion nanoparticles for anti-counterfeit applications. *Nanoscale*. 2015;7(10):4423–31.
- Meruga JM, Baride A, Cross W, et al. Red-green-blue printing using luminescence-upconversion inks. *J Mater Chem C*. 2014;2(12):2221–7.
- Meruga JM, Cross WM, Stanley May P, et al. Security printing of covert quick response codes using upconverting nanoparticle inks. *Nanotechnology*. 2012;23(39):395201.
- Kim WJ, Nyk M, Prasad PN. Color-coded multilayer photopatterned microstructures using lanthanide (III) ion co-doped NaYF₄ nanoparticles with upconversion luminescence for possible applications in security. *Nanotechnology*. 2009;20(18):185301.
- Duan C, Liang L, Li L, et al. Recent progress in upconversion luminescence nanomaterials for biomedical applications. *J Mater Chem B*. 2018;6(2):192–209.
- Gnach A, Lipinski T, Bednarkiewicz A, et al. Upconverting nanoparticles: assessing the toxicity. *Chem Soc Rev*. 2015;44(6):1561–84.
- Sun L, Wei Z, Chen H, et al. Folic acid-functionalized up-conversion nanoparticles: toxicity studies in vivo and in vitro and targeted imaging applications. *Nanoscale*. 2014;6(15):8878–83.
- Boyer J-C, Carling C-J, Gates BD, et al. Two-way photoswitching using one type of near-infrared light, upconverting nanoparticles, and changing only the light intensity. *J Am Chem Soc*. 2010;132(44):15766–72.
- Jones CE, Mackay RA. Reactions in microemulsions. 3. Photodegradation of chlorophyll. *J Phys Chem*. 1978;82(1):63–5.
- Zhang F, Shi Q, Zhang Y, et al. fluorescence upconversion microbarcodes for multiplexed biological detection: nucleic acid encoding. *Adv Mater*. 2011;23(33):3775–9.
- Blumenthal T, Meruga J, Stanley MP, et al. Patterned direct-write and screen-printing of NIR-to-visible upconverting inks for security applications. *Nanotechnology*. 2012;23(18):185305.
- Tong X, Xiang J, Lu X, et al. Electrically enhancing and modulating the photoluminescence of upconversion nanoparticles using liquid crystals. *J Mater Chem C*. 2018;6(28):7683–8.
- Tong X, Xiang J, Shi F, et al. Near-infrared light-sensitive supramolecular gel with enhanced visible light upconversion. *Adv Opt Mater*. 2016;4(9):1392–6.
- Dong A, Ye X, Chen J, et al. A generalized ligand-exchange strategy enabling sequential surface functionalization of colloidal nanocrystals. *J Am Chem Soc*. 2011;133(4):998–1006.
- Cunningham MF, Campbell JD, Fu Z, et al. Future green chemistry and sustainability needs in polymeric coatings. *Green Chem*. 2019;21(18):4919–26.
- Wang C, Wu J, Li L, et al. A facile preparation of a novel non-leaching antimicrobial waterborne polyurethane leather coating functionalized by quaternary phosphonium salt. *J Leather Sci Eng*. 2020;2(1):2.

43. Han Y, Hu J, Xin Z. Facile preparation of high solid content waterborne polyurethane and its application in leather surface finishing. *Prog Org Coat.* 2019;130:8–16.
44. Wen J, Sun Z, Fan H, et al. Synthesis and characterization of a novel fluorinated waterborne polyurethane. *Prog Org Coat.* 2019;131:291–300.
45. Kang S-Y, Ji Z, Tseng L-F, et al. Design and synthesis of waterborne polyurethanes. *Adv Mater.* 2018;30(18):1706237.
46. Chattopadhyay DK, Raju KVS. Structural engineering of polyurethane coatings for high performance applications. *Prog Polym Sci.* 2007;32(3):352–418.
47. Lin J, Ma H, Wang Z, et al. 808 nm near-infrared light-triggered payload release from green light-responsive donor–acceptor stenhouse adducts polymer-coated upconversion nanoparticles. *Macromol Rapid Commun.* 2021;42(19):2100318.
48. Damasco JA, Chen G, Shao W, et al. Size-tunable and monodisperse Tm^{3+}/Gd^{3+} -doped hexagonal $NaYbF_4$ nanoparticles with engineered efficient near infrared-to-near infrared upconversion for in vivo imaging. *ACS Appl Mater Interfaces.* 2014;6(16):13884–93.
49. Wang G, Peng Q, Li Y. Upconversion luminescence of monodisperse $CaF_2:Yb^{3+}/Er^{3+}$ nanocrystals. *J Am Chem Soc.* 2009;131(40):14200–1.
50. Krämer KW, Biner D, Frei G, et al. Hexagonal sodium yttrium fluoride based green and blue emitting upconversion phosphors. *Chem Mater.* 2004;16(7):1244–51.
51. Wu S, Butt H-J. Near-infrared-sensitive materials based on upconverting nanoparticles. *Adv Mater.* 2016;28(6):1208–26.
52. Lai J, Zhang Y, Pasquale N, et al. An upconversion nanoparticle with orthogonal emissions using dual NIR excitations for controlled two-way photoswitching. *Angew Chem Int Ed.* 2014;53(52):14419–23.
53. Zhang X, Guo Z, Zhang X, et al. Mass production of poly(ethylene glycol) monooleate-modified core-shell structured upconversion nanoparticles for bio-imaging and photodynamic therapy. *Sci Rep.* 2019;9(1):5212.
54. Navarro D, Wu J, Lin W, et al. Life cycle assessment and leather production. *J Leather Sci Eng.* 2020;2(1):26.
55. Wang Y, Liu Z, Zhou C, et al. A facile strategy for high performance recyclable polymer systems via dynamic metal ion crosslinking. *J Mater Chem A.* 2019;7(8):3577–82.

Publisher's Note

Springer Nature remains neutral with regard to jurisdictional claims in published maps and institutional affiliations.

Submit your manuscript to a SpringerOpen[®] journal and benefit from:

- Convenient online submission
- Rigorous peer review
- Open access: articles freely available online
- High visibility within the field
- Retaining the copyright to your article

Submit your next manuscript at ► [springeropen.com](https://www.springeropen.com)
